



# Relationship between pulmonary blood flow and volume following lung resection using dynamic perfusion digital radiography

Jun Hanaoka<sup>1^</sup>, Kazuki Hayashi<sup>2^</sup>, Takuya Shiratori<sup>1^</sup>, Keigo Okamoto<sup>1^</sup>, Yoko Kataoka<sup>1^</sup>, Yo Kawaguchi<sup>1^</sup>, Yasuhiko Ohshio<sup>1^</sup>, Akinaga Sonoda<sup>3^</sup>

<sup>1</sup>Division of General Thoracic Surgery, Department of Surgery, Shiga University of Medical Science, Otsu, Japan; <sup>2</sup>Department of General Thoracic Surgery, Omi Medical Center, Kusatsu, Japan; <sup>3</sup>Department of Radiology, Shiga University of Medical Science, Otsu, Japan

*Contributions:* (I) Conception and design: J Hanaoka; (II) Administrative support: A Sonoda; (III) Provision of study materials or patients: J Hanaoka, K Hayashi, T Shiratori, K Okamoto, Y Kataoka, Y Kawaguchi, Y Ohshio; (IV) Collection and assembly of data: J Hanaoka; (V) Data analysis and interpretation: J Hanaoka, K Hayashi, T Shiratori; (VI) Manuscript writing: All authors; (VII) Final approval of manuscript: All authors.

*Correspondence to:* Jun Hanaoka, MD, PhD. Division of General Thoracic Surgery, Department of Surgery, Shiga University of Medical Science, Tsukinowacho, Otsu, Shiga 520-2192, Japan. Email: hanaoka@belle.shiga-med.ac.jp.

**Background:** Surgical intervention for lung resection can cause ventilation-perfusion mismatches and affect gas exchange; however, minimally invasive assessment of blood flow is difficult. This study aimed to evaluate changes in pulmonary blood flow after radical lung cancer surgery using a minimally invasive dynamic digital chest radiography system.

**Methods:** We evaluated 64 patients who underwent radical lobectomies. Postoperative changes in pulmonary blood flow, assessed using dynamic chest radiography-based blood flow ratios (BFRs), were compared with the temporal evolution of both functional lung volumes (FLVs) and estimated lung weight (ELW) derived from computed tomography (CT) volumetry.

**Results:** FLVs on the affected side gradually recovered over time from the lowest value observed 3 months after surgery in all procedures. BFRs on the affected side also showed a gradual recovery from the lowest value 1 month after surgery, except for left upper lobectomies (LULs). In LULs, FLVs and ELWs increased proportionally up to 3 months after surgery, with lung volumes continuing to increase thereafter. The recovery of BFRs differed depending on the resected lobe.

**Conclusions:** A relationship between pulmonary blood flow and FLV was observed in the postoperative period. Despite varying compensatory responses depending on the surgical procedure, FLV recovery coincided with increased pulmonary blood flow.

**Keywords:** Dynamic perfusion digital radiography (DPDR); dynamic chest radiography; pulmonary blood flow; functional lung volume (FLV); lung cancer

Submitted Jun 21, 2023. Accepted for publication Sep 14, 2023. Published online Oct 08, 2023.

doi: 10.21037/jtd-23-986

**View this article at:** <https://dx.doi.org/10.21037/jtd-23-986>

<sup>^</sup> ORCID: Jun Hanaoka, 0000-0002-5272-556X; Kazuki Hayashi, 0000-0002-2393-1233; Takuya Shiratori, 0009-0002-5056-7112; Keigo Okamoto, 0000-0002-6992-3765; Yoko Kataoka, 0000-0001-6268-6587; Yo Kawaguchi, 0000-0002-7828-4635; Yasuhiko Ohshio, 0009-0008-4682-0350; Akinaga Sonoda, 0000-0003-2410-6232.

## Introduction

Lobectomies for early-stage non-small-cell lung cancer can result in a reduction in lung volume and anatomical changes due to intrathoracic dead space. These changes may cause ventilatory disorders, including tracheobronchial tree deviation or torsion, and reduced blood flow (1,2), leading to ventilation-perfusion mismatches and impaired gas exchange (3). While airway deviation can be observed using bronchoscopy and imaging, minimally invasive assessment of blood flow is challenging (4).

Conventionally, three-dimensional (3D) computed tomography (CT), pulmonary arteriography, and pulmonary perfusion scintigraphy (PPS) are used for observing pulmonary perfusion; however, their repeatability is limited owing to ionizing radiation exposure (5). Among non-radiation examinations, magnetic resonance imaging (MRI) has enabled morphological and respiratory physiological evaluation using ventilation, lung perfusion, and pulmonary function imaging (6). However, these methods are limited to certain facilities because of constraints, including equipment cost and examination time. Therefore, other minimally invasive procedures that are easily accessible are warranted.

Dynamic perfusion digital radiography (DPDR) uses dynamic chest radiography (DCR) to evaluate pulmonary blood flow distribution without contrast agents. DPDR

provides a qualitative blood flow evaluation using color-coded changes in pixel values and quantitative evaluations regarding the left-right blood flow ratio (BFR) (7,8). In a previous study (9), a strong association was found between the extent of alterations in pixel values and the level of blood circulation in the lungs in animal experiments. Additionally, a significant correlation was observed between the calculated left and right BFR using the method employed in the study and PPS results (8,10). DPDR is useful for diagnosing chronic thromboembolic pulmonary hypertension (CTEPH) (11), distinguishing between pulmonary arterial and CTEPH (12), and evaluating thrombus reduction assessment (13). DCR and standard chest radiography can be performed simultaneously owing to similar setups. DPDR provides a noninvasive diagnosis for patients with contraindications to angiography, making it suitable for preoperative screening and postoperative follow-up. Its minimal invasiveness and repeatability are advantageous for clinical use, even during periods when postoperative effects may hinder sufficient evaluation through spirometry.

The aim of this study was to compare the effects of changes in pulmonary blood flow associated with lobectomies for lung cancer, specifically investigating whether these effects are solely attributed to volume reduction or are influenced by anatomical changes, utilizing the differences in anatomical effects among different surgical techniques for comparison. We present this article in accordance with the STROBE reporting checklist (available at <https://jtd.amegroups.com/article/view/10.21037/jtd-23-986/rc>).

## Methods

### Patients

In total, 100 patients scheduled for radical primary lung cancer resection at Shiga University of Medical Science between May 2018 and December 2020 who met the criteria were enrolled in this cohort study. Only patients who could follow breathing instructions involving breath-holding or forced breathing in a sitting position were included. Patients with a history of thoracic surgery, those aged <20 years, and those at risk of adverse events due to irradiation were excluded. Eleven patients were excluded because of other diseases, sublobar resections, and refusal of informed consent during the postoperative period. The final analysis included 64 patients (*Figure 1*), excluding patients

### Highlight box

#### Key findings

- In postoperative observations, compensatory responses varied depending on the surgical procedure, with the exception of left upper lobectomy (LUL), while recovery of functional lung volume (FLV) occurred concomitantly with increased pulmonary blood flow.

#### What is known and what is new?

- Although residual lung volume after surgery has been reported to gradually recover over time, regardless of the surgical procedure, the recovery of postoperative blood flow remains unclear.
- Although a positive correlation was found between blood flow rate and FLV ratio, this correlation gradually diminished after LUL, suggesting the possibility of excessive expansion associated with increased blood flow and lung weight after three months postoperatively.

#### What is the implication, and what should change now?

- The location of the resected lobe has an impact on both blood flow and volume recovery, and understanding whether this recovery discrepancy affects postoperative gas exchange and perioperative management is a critical research challenge.

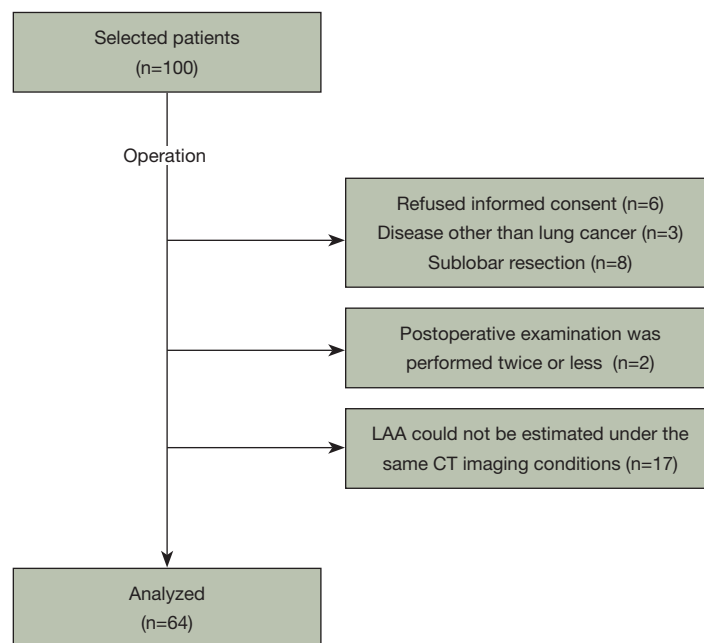


**Figure 1** Flow diagram of the study. The final analysis was performed on 64 patients with LAA in three or more postoperative examinations under the same CT imaging conditions. LAA, low-attenuation area; CT, computed tomography.

with fewer than two postoperative examinations ( $n=2$ ) and patients in whom low-attenuation area (LAA) estimation was not possible under the same CT imaging conditions ( $n=17$ ).

The study was conducted in accordance with the Declaration of Helsinki (as revised in 2013). The study was approved by the institutional review board of Shiga University of Medical Science (CRB 5180008; October 10, 2017) and written informed consent was taken from all individual participants. This study was registered as a clinical trial (UMIN000029716).

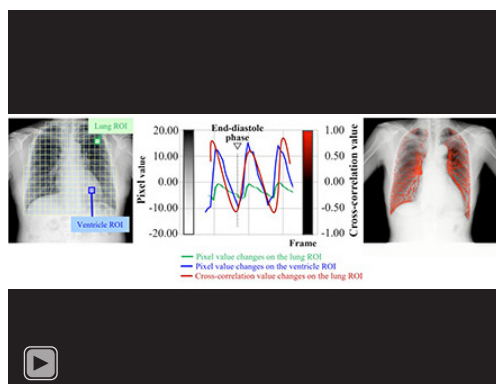
### **Imaging protocol for DCR**

A prototype dynamic imaging system (Konica Minolta, Inc., Tokyo, Japan) composed of an indirect-conversion flat-panel detector (PaxScan, 4343CB, Varex Imaging Corporation, Salt Lake City, UT, USA), an X-ray tube (RAD-94/B-130H, Varian Medical Systems, Inc., Palo Alto, CA, USA), and a pulsed X-ray generator (EPS45RF, EMD Technologies, Saint-Eustache, Canada). All participants were scanned in a sitting position at a pulse rate of 15 frames/s during breathing patterns, regulated by automated voice guidance. The exposure conditions were as follows: tube voltage, 100 kV; tube current, 40 mA; duration of pulsed X-ray,

5 ms; source-to-image distance, 2 m; an additional filter, 0.5 mm Al + 0.1 mm Cu.

### **BFR measurement from pulmonary perfusion analysis using DCR**

Pulmonary perfusion analysis using DCR was used preoperatively and at 1, 3, 6, and 12 months after surgery, as previously reported (8,10). In detail, pulmonary perfusion was analyzed using dynamic images taken during breath-holding at a resting inspiratory level for 7 s using the cross-correlation method. This process first extracts changes in the pixel values of regions of interest set in arbitrary lung fields and ventricular regions. After removing the pixel value changes corresponding to the respiratory cycle with a high-pass filter, the cross-correlation value was calculated from the degree of waveform correlation between the changes in the pixel values in the pulmonary and ventricular regions. As such, the temporal variation in pixel values of the ventricular region should be the reciprocal of that in the lung field. The pulmonary blood flow was visualized by color-coding the correlation values over the entire lung field. After computing the maximum cross-correlation value (MaxCCv) for each pixel over all frames, the BFR was calculated as the ratio of the sum of the MaxCCv on



**Video 1** Pulmonary perfusion imaging. Pulmonary perfusion was evaluated by visualizing the degree of waveform correlation between the pixel value changes in the lung regions and periodic pixel value changes corresponding to the cardiac cycle using cross-correlation calculation processing. As such, the temporal variation in pixel values of the ventricular region should be the reciprocal of that in the lung field. The cross-correlation value changes are displayed in red in each frame of the chest dynamic image.

the affected side to the sum of the MaxCCv in both the left and right lung fields (*Video 1*). Changes in postoperative pulmonary blood flow were evaluated as the ratio of the affected to the unaffected side.

### CT examinations

Non-contrasted chest CT images were acquired with participants in a supine position preoperatively and at 3, 6, and 12 months after surgery using an Aquilion ONE 80-detector CT scanner (Canon Medical Systems Corporation, Tochigi, Japan) with breath-holding at the end of inspiration. Contiguous 0.5-mm-thick images covering the entire lung were obtained using the following CT parameters: 0.5 s gantry rotation, 80 mm × 0.5 mm detector configuration, 0.637 pitch, 512×512-pixel resolution, and 120 kV tube energy with a variable mA setting using CT-automatic exposure control (standard deviation, 12). These images were reconstructed using a standard lung reconstruction algorithm (FC 52) for volumetric analysis.

### Lung volume measurement

The volume of each territory on the 3D lung model was reconstructed using the image analysis system SYNAPSE VINCENT (ver. 4.3.0001; FUJIFILM Corporation, Tokyo, Japan), using thin-slice CT data. The volumes of the trachea,

bronchi, pulmonary arteries, pulmonary veins, tumors, and other parenchymal structures were semiautomatically and selectively removed from this 3D lung model. We defined functional lung volume (FLV) as the volume obtained by excluding the LAA, which has the lowest attenuation, using a threshold of <-950 Hounsfield units (14), from the total lung volume affected by emphysema. The separation of lung lobes was initiated with automated tracing, the appropriate areas were manually retraced to ensure accuracy. Two or more observers were present to monitor and indicate if modifications were necessary.

The change in postoperative FLV was evaluated using the ratio of the change in postoperative to preoperative volume [FLV change ratio (FLVCR)] and the ratio of the volume of the affected side to the whole volume [FLV ratio (FLVR)].

### Calculation of radiologic lung density and estimated lung weight (ELW)

Lung weights were calculated using lung volumes and mean Hounsfield values automatically obtained from the SYNAPSE VINCENT. ELWs were calculated as follows:

$$\text{ELW} = \text{lung volume (mL)} \times \text{average radiologic lung density (g/mL)} \quad [1]$$

The average radiologic lung density was calculated based on the linear relationship between the Hounsfield value and actual density, as indicated by the following equation (15):

$$\text{Average radiologic lung density} = \frac{\text{mean Hounsfield value} + 1000}{1000} \quad [2]$$

### Statistical analyses

Statistical analyses were performed with EZR (Saitama Medical Center, Jichi Medical University, Saitama, Japan), a graphical user interface for R version 4.0.3 (R Foundation for Statistical Computing, Vienna, Austria). Missing values, which accounted for less than 5% of the total dataset, were handled by leaving those data points blank. This ensured that our statistical analyses were conducted on a dataset with a high level of completeness, minimizing the potential impact of missing data on our findings. Data are reported as mean ± standard deviation. The Wilcoxon signed-rank test with continuity correction was used to compare preoperative and postoperative changes over time in the blood flow percentage FLV on the affected side relative to the whole lung. Moreover, a nonparametric test was

performed using Spearman's rank correlation coefficient to determine the correlation between the ratio of blood flow and FLV on the affected side. All statistical analyses were two-tailed, with a significance threshold of 0.05.

## Results

### *Clinical characteristics*

Table 1 shows the clinical characteristics of the 64 patients from their electronic medical records. Data from this patient population were used in two other related studies (8,10). All patients were followed up 1-year post-surgery. The average age was 72.22 years, with 50 (78.1%) males. Most patients with respiratory comorbidities had a chronic obstructive pulmonary disease (COPD) treatment history. However, among 33 cases with forced expiratory volume in 1 second (FEV1)% <70% on spirometry, 14 had stage II COPD. Video-assisted thoracoscopic surgery (VATS) was the most common surgical approach, with right upper lobectomy (RUL) the most frequent surgery performed, followed by left upper lobectomy (LUL). Respiratory and cardiovascular complications of Clavien-Dindo classification  $\geq$  grade II occurred within 90 days following surgery in 23 and 9 patients, respectively.

### *Changes in postoperative pulmonary BFR*

Figure 2 depicts the changes in the affected BFR following each lobectomy, with Table S1 presenting the corresponding numerical values. The mean preoperative right BFR for all patients was  $0.542 \pm 0.029$ . Although the BFR decreased 1 month postoperatively for both left and right lobectomies, it gradually recovered after right lobectomies, whereas the recovery was poor after left lobectomies (Figure 2A). The comparable recovery of BFR after bilateral lower lobectomy indicates that the recovery of LUL was inferior to that of RUL (Figure 2B). However, although recovery of BFR was observed after RUL, the postoperative BFR was similar to that after right lower lobectomy (RLL), indicating a significant decrease in BFR following RUL compared to the resection volume (Table S1).

### *Changes in FLVCR after each lobectomy*

We compared the changes in FLVCR after lobectomy in the left and right lungs (Figure 3) and in the residual lung lobes on the affected side (Figure S1). After all lobectomies,

lung volume on the healthy side increased within 3 months and then plateaued. The residual lung volume change rate after upper lobectomy gradually increased, with variability on both sides, whereas the residual lung volume after lower lobectomy showed only an increasing tendency. Notably, the middle lobe volume after RUL did not increase compared to after RLL but decreased. Conversely, the residual lower lobe after LUL showed a marked increase.

### *Changes in postoperative FLVR*

Figure 4 shows the changes in affected FLVR after each lobectomy, and Table S2 presents the actual values. The mean preoperative right FLVR in all patients was  $0.542 \pm 0.022$ . After both left and right lobectomies, the FLVR of the affected side decreased 3 months after surgery and then gradually recovered within 3–12 months after surgery, albeit with differences in degrees (Figure 4A). For each lobectomy, the FLVR increased 6 and 12 months after surgery compared to 3 months after surgery (Figure 4B–4D, 4F).

### *Relationship between changes in pulmonary blood flow and FLV after surgery*

We analyzed the correlation between pulmonary BFR and FLVR based on the surgical procedure for all measurements taken from postoperative months 3–12 (Table 2). A positive correlation with  $r$  value  $>0.6$  was observed in all surgical procedures.

Furthermore, we investigated the temporal relationship between the pulmonary BFR and FLVR change rates after LUL and RUL in a relatively large number of patients (Table 3). While a consistent correlation was sustained throughout the observation period after RUL, the correlation gradually disappeared after LUL.

### *Changes in ELW of the residual left lower lobe after LUL*

We compared the changes in the FLV and ELW in the residual left lower lobe to investigate the cause of the discrepancy between lung blood flow and lung volume recovery after LUL (Figure 5, Table S3). In healthy lungs, the FLV and ELW change rates showed similar patterns. Conversely, in the residual left lower lobe after an LUL, both the FLV and ELW increased in parallel up to 3 months after surgery, after which the ELW leveled off, whereas the FLV increased up to 1.4-fold.



**Table 1** Clinical characteristics of the patients

Variables	Value (n=64)
Age (years)	72.22±6.91
Sex	
Male	50 (78.1)
Female	14 (21.9)
Performance status	
0	61 (95.3)
1	3 (4.7)
Affected side	
Right	40 (62.5)
Left	24 (37.5)
Respiratory comorbidities	
Yes	14 (21.9)
COPD	12 (18.8)
BA	1 (1.6)
IP	1 (1.6)
OSAS	1 (1.6)
Circulatory comorbidities	
Yes	35 (54.7)
HT	30 (46.9)
AP	6 (9.4)
Arrhythmia	7 (10.9)
Valvular disorder	2 (3.1)
Others	3 (4.7)
COPD stage	
0	31 (48.4)
1	19 (29.7)
2	14 (21.9)
3	0 (0.0)
Histology	
Adenocarcinoma	50 (78.1)
Squamous cell carcinoma	10 (15.6)
Others	4 (6.3)
Approach	
Open thoracotomy	13 (20.3)
VATS	51 (79.7)

**Table 1** (continued)**Table 1** (continued)

Variables	Value (n=64)
Resected lobe of the lung	
Right upper	26 (40.6)
Right middle	4 (6.3)
Right lower	10 (15.6)
Left upper	14 (21.9)
Left lower	10 (15.6)
Pathological staging	
0	1 (1.6)
IA1	11 (17.2)
IA2	18 (28.1)
IA3	7 (10.9)
IB	11 (17.2)
IIA	2 (3.1)
IIB	8 (12.5)
IIIA	6 (9.4)
Adjuvant therapy	
Yes	16 (25.0)
No	48 (75.0)
Respiratory complications	
Yes	23 (35.9)
Atelectasis	7 (10.9)
Hypoxemia on effort	3 (4.7)
Pleuritis	6 (9.4)
Pneumonia	4 (6.3)
Acute exacerbation of interstitial pneumonia	2 (3.1)
Chylothorax	1 (1.6)
Prolonged lung fistula	1 (1.6)
Circulatory complications	
Yes	9 (14.1)
Arrhythmia	9 (14.1)
LTOT	
Yes	4 (6.3)
No	60 (93.8)

Data are presented as mean ± standard deviation or n (%). COPD, chronic obstructive pulmonary disease; BA, bronchial asthma; IP, interstitial pneumonia; OSAS, obstructive sleep apnea syndrome; HT, hypertension; AP, angina pectoris; VATS, video-assisted thoracic surgery; LTOT, long-term oxygen therapy.

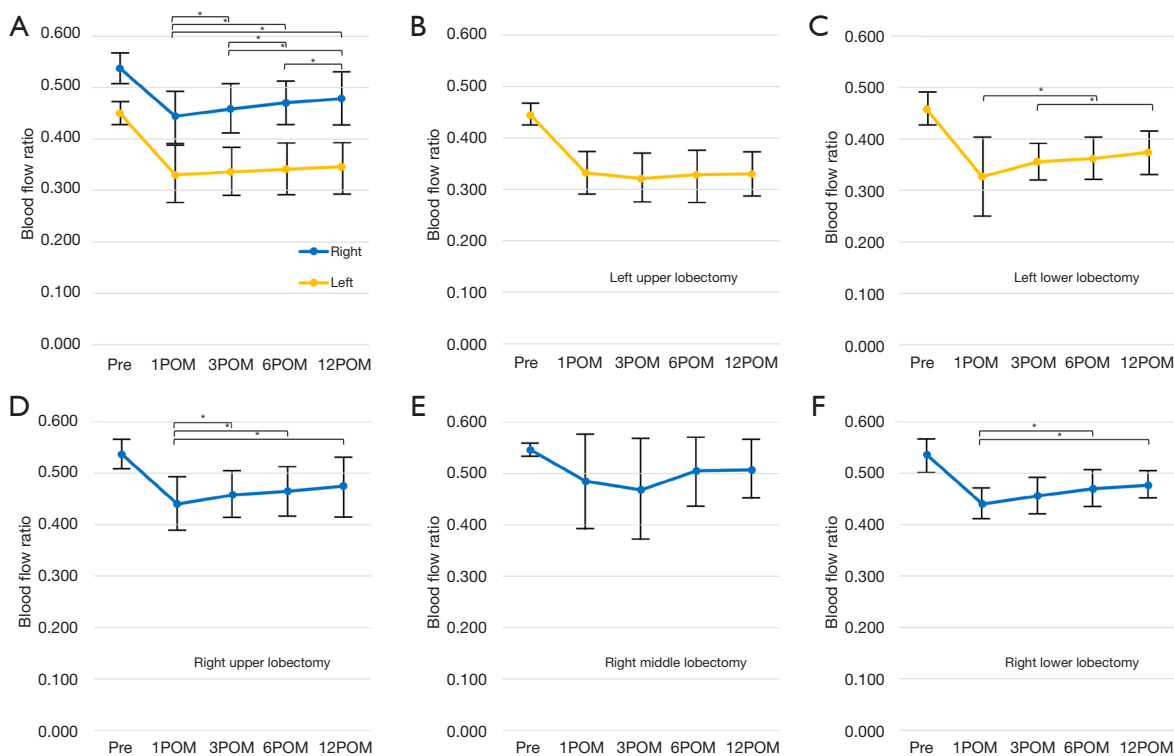


**Figure 2** Changes in pulmonary BFR after each lobectomy. Each line graph shows the following postoperative results by lobectomy site: (A) comparison of left and right, (B) left upper, (C) left lower, (D) right upper, (E) right middle, and (F) right lower. The number of patients with middle lobectomies was small; therefore, there was large variability. Except for LULs, the BFR of the affected side was restored after all surgical procedures. \*,  $P < 0.05$ . The error bars in the figure represent the mean  $\pm$  standard deviation. Pre, preoperative; POM, postoperative months; BFR, blood flow ratio; LUL, left upper lobectomy.

## Discussion

This study investigated the relationship between changes in BFR assessed by DPDR and the FLV calculated from CT images after lobectomies. The residual lung on the affected side showed gradual but incomplete recovery of blood flow and FLV after 1 year, with recovery differing based on the resected lobe. Upper lobectomies resulted in greater loss of FLV than expected; however, residual lung recovery was better than after lower lobectomies. After LULs, there was a discrepancy between blood flow and FLV recovery, with FLV increasing more than blood flow.

Previous studies have utilized 3D-CT volumetry with a specialized lung analysis workstation (16,17) to investigate lung volume changes after surgery. Lung volumes typically sharply decrease in the first postoperative month, then rapidly recover over the next 3 months, and gradually increase from months 3 to 6 (17). Notably, residual lung volume after RLL showed the greatest increase among

all surgeries (16). On the other hand, pulmonary blood flow distributions have mainly been evaluated qualitatively and semi-quantitatively by PPS; however, reports on postoperative blood flow changes are few. Dual-energy CT (DECT) evaluation, which provides simultaneous information on pulmonary anatomy and perfusion (18), revealed the greatest volume and blood flow increases in the affected residual lung 6 months after surgery, regardless of the surgical approach and procedure, except for RLL (19). However, the impact of the resected lobe on blood flow recovery remains to be determined, despite the gradual recovery of lung volume over time.

Postoperative lung capacity and pulmonary blood flow recovery depend on several factors, including vascular bed reduction and anatomical changes related to dead space on the affected side, such as mediastinal deviation, bronchi or pulmonary vessel bending, and diaphragm elevation (2,20). In a previous study (21), lower lobectomy was not inferior to upper lobectomy in terms of functional lung

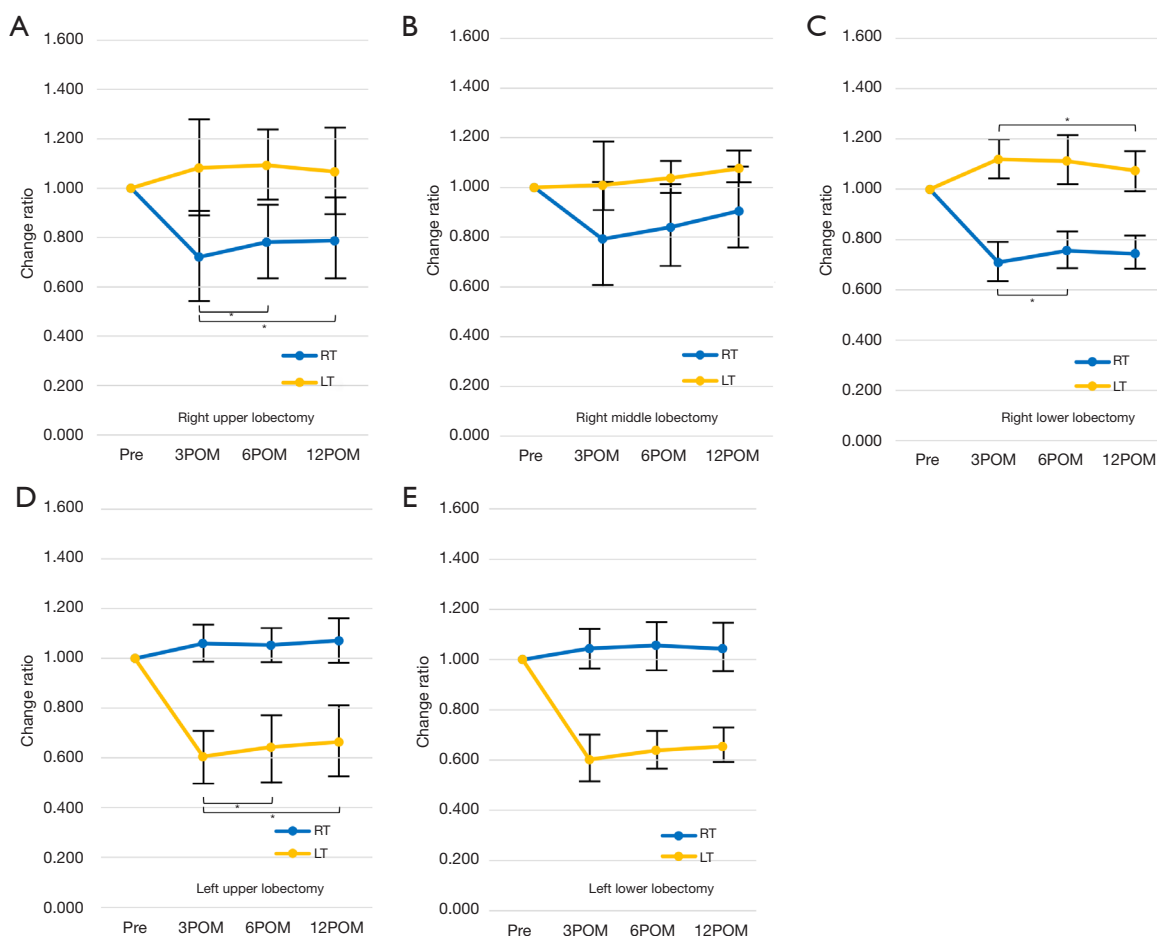


**Figure 3** Postoperative FLVCR after each lobectomy. Each line graph shows the following postoperative results by lobectomy site: (A) right upper, (B) right middle, (C) right lower, (D) left upper, and (E) left lower. \*,  $P < 0.05$ . The error bars in the figure represent the mean  $\pm$  standard deviation. RT, right; LT, left; pre, preoperative; POM, postoperative months; FLVCR, functional lung volume change ratio.

capacity loss on spirometry, despite larger resected lung volumes. The extent of residual lung deviation affects the differences in recovery after upper and lower lobectomies. The residual lung position after lower lobectomy does not change significantly, whereas after upper lobectomy, it displaces cranially. In RUL, the posterosuperior deviation of the middle lobe can cause bronchial stenosis. Alleviating displacement of the right lower lobe by keeping the middle lobe aerated may result in better lung volume and blood flow recovery compared to LUL. In this study, we postulated that the variation in blood flow recovery may be attributed to the differences in volume recovery of the right middle lobe after RUL.

After lung surgery, compensatory lung growth (CLG) can improve lung function beyond expectations (22). Lung weight measurements are used to evaluate CLG development (23).

An increase in volume without accompanying weight gain indicates hyperinflation, whereas an increase in weight without volume gain suggests congestion (24), neither of which revealed a significant increase in pulmonary blood flow over time. An increase in lung weight and volume during CLG is believed to involve an increase in pulmonary blood flow. While the observed correlation between BFR and FLVR across all lobectomies in this study may be related to CLG, the possibility of hemodynamic adaptation through the capillaries during the first year after surgery should also be considered (25).

The correlation between the BFR and FLVR was maintained after RUL but gradually decreased after LUL. This occurred because the weight and volume of the left lower lobe increased proportionally until 3 months after the surgery; however, after that, the hyperinflated



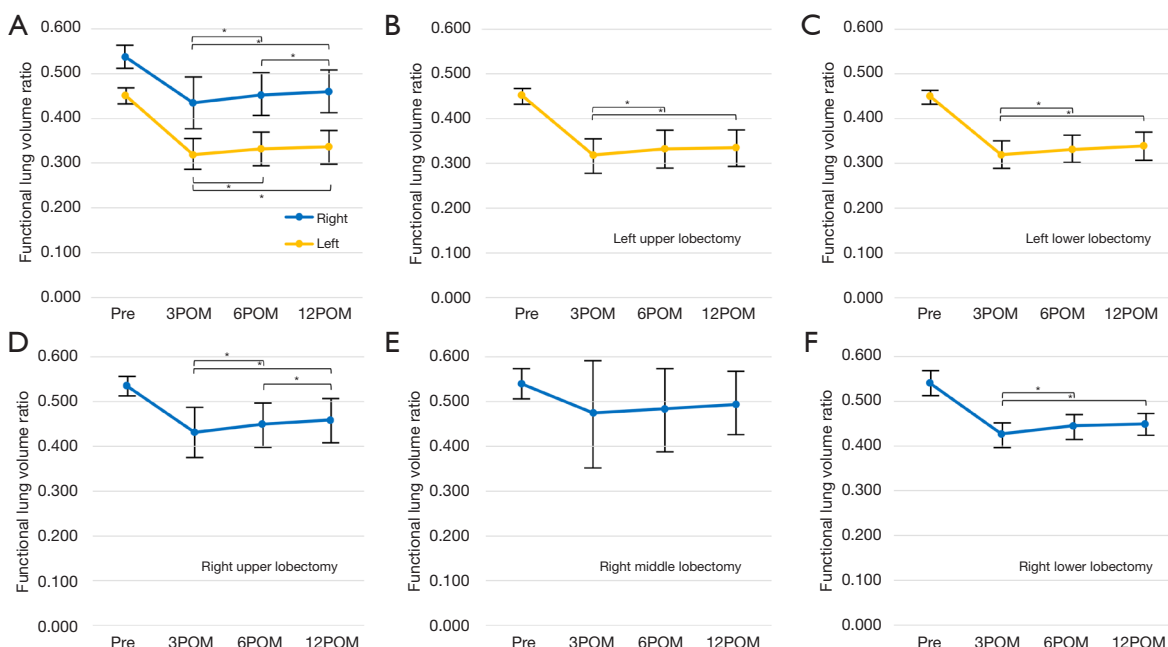


**Figure 4** Changes in FLVR after each lobectomy. Each line graph shows the following postoperative results by lobectomy site: (A) comparison of left and right, (B) left upper, (C) left lower, (D) right upper, (E) right middle, and (F) right lower. The number of patients with middle lobectomies was small; therefore, there was large variability. The FLVR on the affected side was restored after all surgeries. \*, P<0.05. The error bars in the figure represent the mean ± standard deviation. Pre, preoperative; POM, postoperative months; FLVR, functional lung volume ratio.

**Table 2** Comparison of correlations between rates of pulmonary blood flow and FLV in the affected side after each lobectomy

Surgical procedures	Correlation coefficient	P value
RUL	0.817	<0.001
RML	0.825	0.002
RLL	0.683	<0.001
LUL	0.623	<0.001
LLL	0.826	<0.001

FLV, functional lung volume; RUL, right upper lobectomy; RML, right middle lobectomy; RLL, right lower lobectomy; LUL, left upper lobectomy; LLL, left lower lobectomy.

state, during which only the volume increased, persisted. Surgical ligation of pulmonary artery branches increases afterload on the affected artery and leads to decreased blood flow (26). During LUL, which requires manipulation of multiple branches, it is particularly affected. Furthermore, visualization of the tracheobronchial tree using 3D-CT revealed that the basal bronchus is constricted after LUL in many patients, suggesting that this stenosis may have caused a check valve mechanism leading to overinflation. These events have been associated with a higher prevalence of respiratory symptoms in many patients following LULs (1,20). The discrepancy observed in the recovery of FLV

**Table 3** Comparison of correlations between rates of pulmonary blood flow and FLV in the affected side after RUL and LUL

Surgical procedures	3POM		6POM		12POM	
	Correlation coefficient	P value	Correlation coefficient	P value	Correlation coefficient	P value
RUL	0.707	<0.001	0.831	<0.001	0.891	<0.001
LUL	0.753	0.004	0.553	0.040	0.524	0.055

FLV, functional lung volume; RUL, right upper lobectomy; LUL, left upper lobectomy; POM, postoperative months.

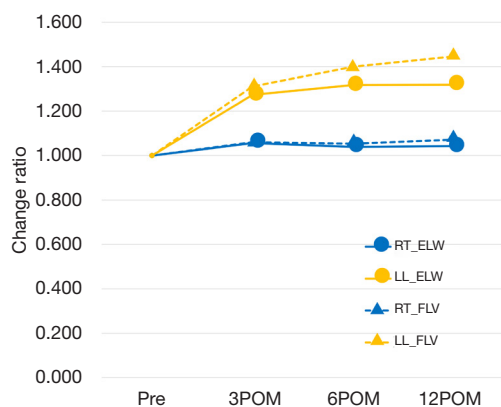


**Figure 5** Changes in FLVs and ELWs in the residual lobe after RUL or LUL. Circles indicate changes in ELWs, and triangles indicate changes in FLVs. RT, right lung; ELW, estimated lung weight; LL, left lower lobe; FLV, functional lung volume; pre, preoperative; POM, postoperative months; RUL, right upper lobectomy; LUL, left upper lobectomy.

and BFR after LUL in our study reflects the negative impact of postoperative anatomical changes, which should be considered a potential cause of impaired gas exchange in other surgical procedures.

The current study had some limitations. Firstly, it was a single-center study with a small sample size, resulting in insufficient patients for adjusting preoperative clinical factors that could impact postoperative outcomes, such as smoking history and respiratory comorbidities. This limits the generalizability of our findings. Secondly, there is the challenge of blind spots during the evaluation of blood flow in the left lung field. DPDR entails a two-dimensional (2D) assessment, which may lead to an underestimation of areas overlapping with cardiac shadows. To date, reports of BFRs utilizing perfusion scintigraphy or MRI have indicated the right-side accounting for 50.5% to 55% (27,28). This study's value of 54.2% does not markedly deviate from these figures. Although our previous studies have reported a high correlation between the BFR and PPS (8,10) measured by the cross-correlation analysis. Further investigations, including correlation with phase-contrast cardiac MRI (7), are necessary to accurately determine the left and right blood flow. Thirdly, DPDR evaluation provides limited information about the blood flow distribution within each lobe because of the constrained direction of dynamic images.

We previously reported on the more accurate prediction

of postoperative complications using preoperative BFRs. This study explored the potential of postoperative changes in BFRs as independent respiratory assessments, separate from FEV recovery. However, the postoperative assessment of practical lung function aims to confirm the maintenance of adequate gas exchange, which is determined by the balance between blood flow and ventilation. Various factors influence blood flow, such as the effect of increased negative pressure in the thoracic cavity on blood flow after lung resection, counteracted by the decrease in vascular bed, as well as differences in gravitational effects based on the type of remaining lung lobes. The assessment of blood flow in this study represents the summation of these contributing factors. DPDR offers visual and quantitative information to analyze the factors behind shortness of breath in postoperative patients, a concern that has been difficult to assess due to challenges in evaluating lung perfusion distribution. As gas exchange evaluation was not performed in this series, future plans involve accumulating case analyses combining symptom progression.

## Conclusions

Our study demonstrated a strong correlation between pulmonary blood flow and FLV during postoperative changes. Early after surgery, the affected lung showed a decreased vascular bed and increased lung volume in the healthy lung, followed by compensatory volume recovery with increased blood flow in the affected lung. Additionally, the location of the resected lung influenced the course of these transitions.

## Acknowledgments

We want to thank Editage (<https://www.editage.jp/>) for the English language editing. Katsunori Miyata, a radiological technician at Shiga University of Medical Science, contributed substantially by assisting with the DCR.

*Funding:* This work was supported by Konica Minolta, Inc.

## Footnote

*Reporting Checklist:* The authors have completed the STROBE reporting checklist. Available at <https://jtd.amegroups.com/article/view/10.21037/jtd-23-986/rc>

*Data Sharing Statement:* Available at <https://jtd.amegroups.com>

[com/article/view/10.21037/jtd-23-986/dss](https://doi.org/10.21037/jtd-23-986/dss)

*Peer Review File:* Available at <https://jtd.amegroups.com/article/view/10.21037/jtd-23-986/prf>

*Conflicts of Interest:* All authors have completed the ICMJE uniform disclosure form (available at <https://jtd.amegroups.com/article/view/10.21037/jtd-23-986/coif>). JH received a research grant from Konica Minolta Inc. The other authors have no conflicts of interest to declare.

*Ethical Statement:* The authors are accountable for all aspects of the work in ensuring that questions related to the accuracy or integrity of any part of the work are appropriately investigated and resolved. The study was conducted in accordance with the Declaration of Helsinki (as revised in 2013). The study was approved by the institutional review board of Shiga University of Medical Science (CRB 5180008; October 10, 2017) and written informed consent was taken from all individual participants.

*Open Access Statement:* This is an Open Access article distributed in accordance with the Creative Commons Attribution-NonCommercial-NoDerivs 4.0 International License (CC BY-NC-ND 4.0), which permits the non-commercial replication and distribution of the article with the strict proviso that no changes or edits are made and the original work is properly cited (including links to both the formal publication through the relevant DOI and the license). See: <https://creativecommons.org/licenses/by-nc-nd/4.0/>.

## References

1. Ueda K, Tanaka T, Hayashi M, et al. Clinical ramifications of bronchial kink after upper lobectomy. *Ann Thorac Surg* 2012;93:259-65.
2. Kim CW, Godelman A, Jain VR, et al. Postlobectomy chest radiographic changes: a quantitative analysis. *Can Assoc Radiol J* 2011;62:280-7.
3. Sekine Y, Miyata Y, Yamada K, et al. Evaluation of pulmonary gas exchange after lobectomy and simple thoracotomy. *Scand Cardiovasc J* 2000;34:339-44.
4. Yanagihara T, Sekine Y, Sugai K, et al. Risk factors of middle lobe bronchus kinking following right upper lobectomy. *J Thorac Dis* 2021;13:3010-20.
5. Johns CS, Swift AJ, Hughes PJC, et al. Pulmonary MR angiography and perfusion imaging-A review of methods and applications. *Eur J Radiol* 2017;86:361-70.
6. Ohno Y, Hanamatsu S, Obama Y, et al. Overview of MRI for pulmonary functional imaging. *Br J Radiol* 2022;95:20201053.
7. Tanaka R. Dynamic chest radiography: flat-panel detector (FPD) based functional X-ray imaging. *Radiol Phys Technol* 2016;9:139-53.
8. Hanaoka J, Shiratori T, Okamoto K, et al. Reliability of dynamic perfusion digital radiography as an alternative to pulmonary perfusion scintigraphy in predicting postoperative lung function and complications. *J Thorac Dis* 2022;14:3234-44.
9. Miyatake H, Tabata T, Tsujita Y, et al. Detection of Pulmonary Embolism Using a Novel Dynamic Flat-Panel Detector System in Monkeys. *Circ J* 2021;85:361-8.
10. Hanaoka J, Yoden M, Hayashi K, et al. Dynamic perfusion digital radiography for predicting pulmonary function after lung cancer resection. *World J Surg Oncol* 2021;19:43.
11. Yamasaki Y, Abe K, Kamitani T, et al. Efficacy of Dynamic Chest Radiography for Chronic Thromboembolic Pulmonary Hypertension. *Radiology* 2023;306:e220908.
12. Yamasaki Y, Kamitani T, Abe K, et al. Diagnosis of Pulmonary Hypertension Using Dynamic Chest Radiography. *Am J Respir Crit Care Med* 2021;204:1336-7.
13. Miyatake H, Asada K, Tabata T, et al. Novel Pulmonary Circulation Imaging Using Dynamic Chest Radiography for Acute Pulmonary Embolism. *Circ J* 2021;85:400.
14. Gevenois PA, De Vuyst P, de Maertelaer V, et al. Comparison of computed density and microscopic morphometry in pulmonary emphysema. *Am J Respir Crit Care Med* 1996;154:187-92.
15. Gattinoni L, Caironi P, Pelosi P, et al. What has computed tomography taught us about the acute respiratory distress syndrome? *Am J Respir Crit Care Med* 2001;164:1701-11.
16. Sengul AT, Sahin B, Celenk C, et al. Postoperative lung volume change depending on the resected lobe. *Thorac Cardiovasc Surg* 2013;61:131-7.
17. Du X, Li H, Liu L, et al. A preliminary study identifies early postoperative lung volume changes in patients with non-small cell lung cancer following video-assisted thoracic surgery using CT volumetry. *Mol Clin Oncol* 2021;14:124.
18. Hong SR, Chang S, Im DJ, et al. Feasibility of Single Scan for Simultaneous Evaluation of Regional Krypton and Iodine Concentrations with Dual-Energy CT: An Experimental Study. *Radiology* 2016;281:597-605.
19. Suh YJ, Lee CY, Lee S, et al. Patterns of Postoperative Changes in Lung Volume and Perfusion Assessed by Dual-

- Energy CT: Comparison of Lobectomy and Limited Resection. *AJR Am J Roentgenol* 2023;220:660-71.
20. Gu Q, Qi S, Yue Y, et al. Structural and functional alterations of the tracheobronchial tree after left upper pulmonary lobectomy for lung cancer. *Biomed Eng Online* 2019;18:105.
  21. Ueda K, Tanaka T, Hayashi M, et al. Compensation of pulmonary function after upper lobectomy versus lower lobectomy. *J Thorac Cardiovasc Surg* 2011;142:762-7.
  22. Hsia CC. Signals and mechanisms of compensatory lung growth. *J Appl Physiol* (1985) 2004;97:1992-8.
  23. Wakamatsu I, Matsuguma H, Nakahara R, et al. Factors associated with compensatory lung growth after pulmonary lobectomy for lung malignancy: an analysis of lung weight and lung volume changes based on computed tomography findings. *Surg Today* 2020;50:144-52.
  24. Waller DA, Keavey P, Woodfine L, et al. Pulmonary endothelial permeability changes after major lung resection. *Ann Thorac Surg* 1996;61:1435-40.
  25. Glénet S, de Bisschop C, Delcambre F, et al. No compensatory lung growth after resection in a one-year follow-up cohort of patients with lung cancer. *J Thorac Dis* 2017;9:3938-45.
  26. Glass A, McCall P, Arthur A, et al. Pulmonary artery wave reflection and right ventricular function after lung resection. *Br J Anaesth* 2023;130:e128-36.
  27. Wieslander B, Ramos JG, Ax M, et al. Supine, prone, right and left gravitational effects on human pulmonary circulation. *J Cardiovasc Magn Reson* 2019;21:69.
  28. Bailey DL, Farrow CE, Lau EM. V/Q SPECT-Normal Values for Lobar Function and Comparison With CT Volumes. *Semin Nucl Med* 2019;49:58-61.

**Cite this article as:** Hanaoka J, Hayashi K, Shiratori T, Okamoto K, Kataoka Y, Kawaguchi Y, Ohshio Y, Sonoda A. Relationship between pulmonary blood flow and volume following lung resection using dynamic perfusion digital radiography. *J Thorac Dis* 2023;15(10):5593-5604. doi: 10.21037/jtd-23-986

**Table S1** Changes over time in the ratio of the affected side to the healthy side of the postoperative pulmonary blood flow distribution

Surgical procedures	Preoperative	1POM	3POM	6POM	12POM
RUL (%)	0.537±0.029	0.440±0.052	0.458±0.045	0.465±0.047	0.475±0.059
RML (%)	0.546±0.013	0.485±0.092	0.468±0.097	0.505±0.066	0.507±0.056
RLL (%)	0.536±0.035	0.440±0.032	0.456±0.036	0.470±0.035	0.477±0.027
Right side (%)	0.537±0.029	0.445±0.053	0.459±0.048	0.470±0.047	0.479±0.052
LUL (%)	0.444±0.023	0.332±0.041	0.321±0.047	0.329±0.050	0.330±0.046
LLL (%)	0.458±0.033	0.327±0.077	0.356±0.036	0.362±0.042	0.374±0.045
Left side (%)	0.450±0.028	0.330±0.055	0.336±0.045	0.342±0.049	0.346±0.050

This table presents the corresponding numerical values at each time point, represented as mean ± standard deviation, depicting the changes in the affected BFR following each lobectomy, as illustrated in Figure 2. POM, postoperative months; RUL, right upper lobectomy; RML, right middle lobectomy; RLL, right lower lobectomy; LUL, left upper lobectomy; LLL, left lower lobectomy; BFR, blood flow ratio.

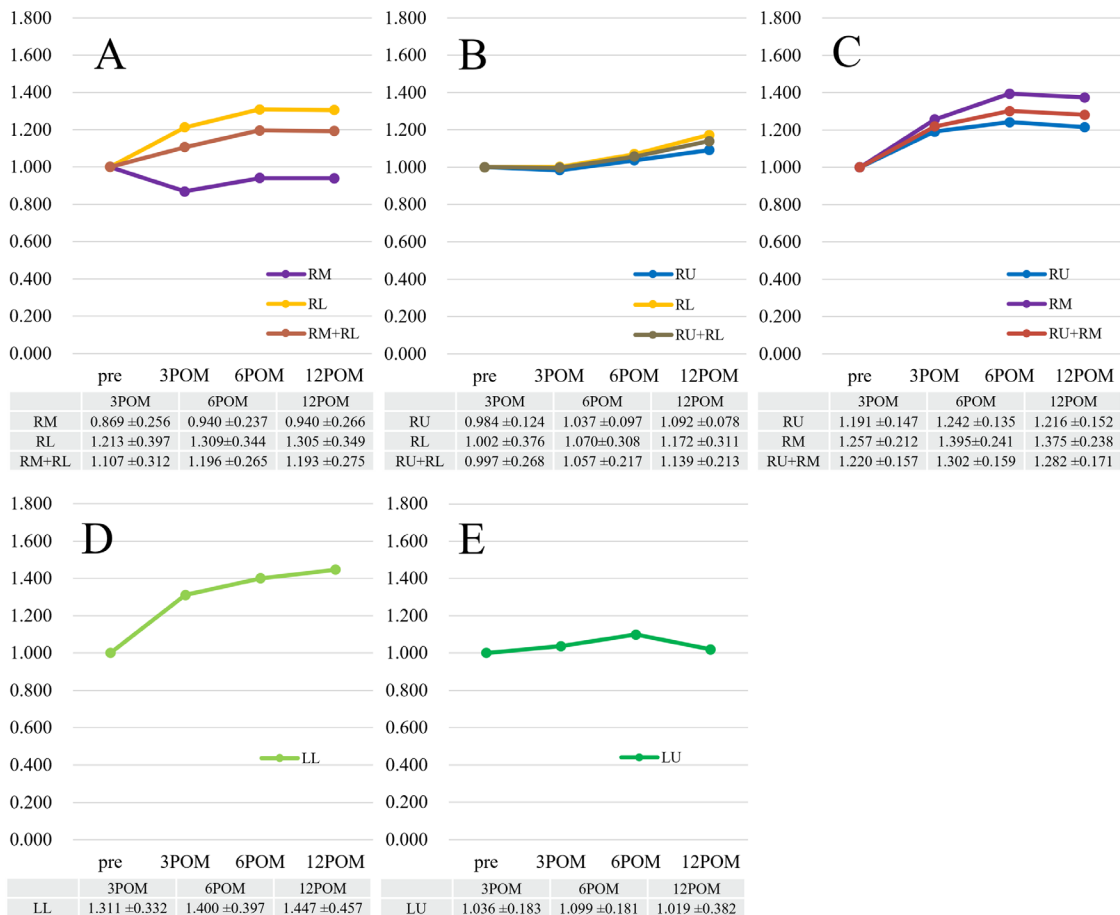


**Figure S1** Transition of changes in FLVR of residual lung lobes in affected side after each lobectomy. Each line graph shows the following postoperative results: (A) RUL, (B) RML, (C) RLL, (D) LUL, and (E) LLL. The sum of the remaining two lobes is also presented, particularly for right-sided surgeries. RM, right middle lobe; RL, right lower lobe; pre, preoperative; POM, postoperative months; RU, right upper lobe; LL, left lower lobe; LU, left upper lobe; FLVR, functional lung volume ratio; RUL, right upper lobectomy; RML, right middle lobectomy; RLL, right lower lobectomy; LUL, left upper lobectomy; LLL, left lower lobectomy.

**Table S2** Changes over time in the ratio of the affected side to the healthy side of the postoperative FLV

Surgical procedures	Preoperative	3POM	6POM	12POM
RUL (%)	0.536±0.022	0.431±0.053	0.450±0.049	0.459±0.049
RML (%)	0.540±0.039	0.475±0.119	0.484±0.092	0.494±0.068
RLL (%)	0.541±0.026	0.427±0.029	0.445±0.027	0.449±0.027
Right side (%)	0.537±0.024	0.435±0.055	0.452±0.049	0.460±0.047
LUL (%)	0.452±0.016	0.319±0.040	0.332±0.042	0.335±0.044
LLL (%)	0.450±0.014	0.319±0.033	0.331±0.030	0.339±0.030
Left side (%)	0.451±0.015	0.319±0.036	0.332±0.037	0.337±0.038

This table presents the corresponding actual values at each time point, represented as mean ± standard deviation, depicting the changes in the affected FLVR after each lobectomy, as illustrated in *Figure 4*. FLV, functional lung volume; POM, postoperative months; RUL, right upper lobectomy; RML, right middle lobectomy; RLL, right lower lobectomy; LUL, left upper lobectomy; LLL, left lower lobectomy; FLVR, functional lung volume ratio.

**Table S3** Temporal evolution of ELW and FLV change rates in the residual left lower lobe following LUL

Parameters	Preoperative	3POM	6POM	12POM
RT_ELW	1.000±0.000	1.056±0.075	1.038±0.051	1.042±0.054
LL_ELW	1.000±0.000	1.273±0.175	1.318±0.213	1.318±0.213
RT_FLV	1.000±0.000	1.060±0.075	1.053±0.072	1.071±0.095
LL_FLV	1.000±0.000	1.300±0.332	1.400±0.397	1.447±0.457

This table presents the corresponding actual values at each time point, represented as mean ± standard deviation, depicting the FLV and ELW changes rate in the residual left lower lobe following LUL, as shown in *Figure 5*. ELW, estimated lung weight; FLV, functional lung volume; LUL, left upper lobectomy; POM, postoperative months; RT, right lung; LL, left lower lobe.